

Recombination coefficients for H_3O^+ ions with electrons e^- and with Cl^- , Br^- and I^- at flame temperatures 1820–2400 K

Jingzhong Guo, John M. Goodings *

Department of Chemistry, Centre for Research in Mass Spectrometry, York University, 4700 Keele Street, Toronto, Ont., Canada, M3J 1P3

Received 28 June 2000; in final form 29 August 2000

Abstract

Rate coefficients were measured for gas-phase electron–ion recombination of H_3O^+ and for ion–ion recombination of H_3O^+ with Cl^- , Br^- and I^- in five $\text{H}_2\text{--O}_2\text{--N}_2$ flames spanning a temperature range 1820–2400 K. A novel, simple and accurate technique was employed involving total positive ion collection at an electrode located a variable distance downstream of the flame reaction zone; a bias voltage was applied between the collection electrode and the metallic burner. The measured values of the recombination coefficients in $\text{cm}^3 \text{ molecule}^{-1} \text{ s}^{-1}$ units are: $(0.0132 \pm 0.0004)T^{-1.37 \pm 0.05}$ for $\text{H}_3\text{O}^+/\text{e}^-$; $(20.8 \pm 0.7)T^{-2.52 \pm 0.16}$ for $\text{H}_3\text{O}^+/\text{Cl}^-$; $(1.01 \pm 0.04)T^{-2.14 \pm 0.07}$ for $\text{H}_3\text{O}^+/\text{Br}^-$; and $(8.82 \pm 0.35)T^{-2.40 \pm 0.12}$ for $\text{H}_3\text{O}^+/\text{I}^-$. © 2000 Elsevier Science B.V. All rights reserved.

1. Introduction

When a hydrogen–oxygen–diluent flame is doped with a hydrocarbon, a super-equilibrium concentration of positive ions and free electrons is produced by chemi-ionization in the bright luminous reaction zone [1,2]. Essentially the only cation emerging into the burnt-gas region downstream is H_3O^+ whose concentration decays by electron–ion recombination. A number of flames can be employed to cover a broad temperature range, e.g., 1820–2400 K in the present case. Recently, Butler and Hayhurst [3] studied the $\text{H}_3\text{O}^+/\text{e}^-$ recombination process in the same flames which we have used here, and obtained a recombination coefficient

$k_{\text{ei}} = (3.6 \pm 0.5)T^{-2.1 \pm 0.7} \text{ cm}^3 \text{ molecule}^{-1} \text{ s}^{-1}$, where T is the temperature in K. The ions were sampled through a nozzle for analysis by a quadrupole mass spectrometer. The sampling process complicates the necessary determination of absolute ion densities. The temperature dependence has been controversial. In five previous determinations, the exponent n in the temperature coefficient T^n of k_{ei} was variously found to have negative [4,5], zero [6,7] and positive [8] values.

When a halogen is introduced in addition, a fraction of the free electrons form negative ions so that ion–ion recombination of H_3O^+ with Cl^- , Br^- and I^- may also be studied. Mass-spectrometric measurements of the recombination coefficients by Burdett and Hayhurst [9] yielded values of $k_{\text{ii}} = (4.1 \pm 1.6) \times 10^{-8}$, $(2.7 \pm 1.0) \times 10^{-8}$, and $(1.2 \pm 0.7) \times 10^{-8} \text{ cm}^3 \text{ molecule}^{-1} \text{ s}^{-1}$ for Cl^- , Br^- and I^- , respectively; somewhat surprisingly, no

*Corresponding author. Fax: +416-736-5936.

E-mail address: goodings@yorku.ca (J.M. Goodings).

dependence of k_{ii} on temperature was found in the range 1810–2570 K. Other mass-spectrometric determinations gave $k_{ii} = (4.2 \pm 1.6) \times 10^{-8} \text{ cm}^3 \text{ molecule}^{-1} \text{ s}^{-1}$ for Cl^- (1800–2600 K) [10] and $(3.0 \pm 1.0) \times 10^{-8} \text{ cm}^3 \text{ molecule}^{-1} \text{ s}^{-1}$ for I^- (2582 K) [11].

Although some of these recombination coefficients have been measured a number of times, both their magnitudes and particularly their dependencies on temperature are still in doubt. We have recently analyzed the current–voltage (i – V) characteristics of weakly ionized flame plasmas at atmospheric pressure in which the current is measured as a function of the voltage applied between a metal burner and a flat metal plate normal to the flame axis [12,13]. When the plate has a moderate negative bias with respect to the burner, a saturation current is collected from which the absolute ion density of the flame plasma at the plate can be easily and accurately determined. Background for an understanding of the characteristics is provided by recent studies of high-pressure plasmas [14,15] based on the pioneering work of Su and Lam [16,17]. We have employed these very simple experimental methods to measure the recombination coefficients of H_3O^+ with e^- , Cl^- , Br^- and I^- for flame temperatures in the range 1820–2400 K. The technique avoids the difficulties and calibration problems associated with mass-spectrometric sampling which can be severe [3,9,10], particularly in the case of iodine [9]. Accordingly, the recombination coefficients are believed to be more accurate than those previously determined.

2. Experimental

The five H_2 – O_2 – N_2 flames employed for these studies have been well-characterized previously, and their relevant properties are given in Table 1. Each is a premixed, flat, laminar, cylindrical flame (cross-sectional area A) of fuel-rich composition burning at atmospheric pressure with the burnt gas downstream of the reaction zone in plug flow (drift velocity v_f). The addition of a very small metered flow of methane CH_4 ($\leq 4.00 \times 10^{-3}$ mol fraction in the burnt gas) produced H_3O^+ ions by chemi-ionization. When desired, negative ions along with H_3O^+ could be produced in the flame by the addition of vapour from a halocarbon of suitable vapour pressure using a gas saturator maintained at 0°C [18]: Cl^- from C_2HCl_3 ; Br^- from $\text{C}_2\text{H}_2\text{Br}_2$; and I^- from $\text{C}_2\text{H}_5\text{I}$. Part of the diluent nitrogen was employed as the carrier gas through the saturator. In the present experiments, any one halocarbon was added to give the same mol fraction of total halogen in the burnt gas of each of the five flames. The mol fractions employed were 4.00×10^{-3} for Cl, and 2.00×10^{-3} for Br and for I.

The very simple apparatus consisted of a water-cooled metallic burner located a variable distance z from a water-cooled metallic plate oriented normal to the flame axis. Both of these electrodes were electrically isolated [12]. The burner which has been described previously [19] consists of a circular bundle of hypodermic tubes mounted in a brass body; the front face of the burner is flat and parallel to the plate. The plate electrode does, in fact, contain the sampling nozzle of our flame-ion mass

Table 1
Properties of the hydrogen–oxygen–nitrogen flames

Property/flame number	2	25	3	4	5
$\text{H}_2/\text{O}_2/\text{N}_2$	2.74/1/2.95	3.0/1/3.5	3.18/1/4.07	3.09/1/4.74	3.12/1/5.77
Measured flame temperature T_f (K)	2400	2230	2080	1980	1820
Cross-sectional area A (10^{-4} m^2)	1.05	1.01	0.993	1.04	0.990
Velocity in the burnt gas v_f (m s^{-1})	19.8	16.2	15.6	11.4	8.4
Mol ratio r , unburnt/burnt gas	1.170	1.152	1.137	1.127	1.112
<i>Equilibrium burnt gas composition (mol fractions)</i>					
H_2O	0.3460	0.3063	0.2754	0.2553	0.2249
H_2	0.1286	0.1527	0.1622	0.1390	0.1259
H	0.006019	0.002650	0.001077	0.0005008	0.0001415
N_2	0.5157	0.5375	0.5610	0.6052	0.6490

spectrometer but that is not relevant in the present application. The plate electrode was biased 50 V negative with respect to the burner, and the net current through the circuit was measured by a sensitive electrometer. In the figures to follow, the measured current indicated is that collected by the plate electrode [12].

The flame is a quasi-neutral plasma; at every point $n_+ = n_e + n_-$, where n is the charge density and the subscripts +, e and – refer to positive ions, electrons and negative ions (if present), respectively [12–15]. The plate electrode is covered by a plasma sheath of positive ions. When the negative bias voltage on the plate is increased from zero, the electrons moving at the flame drift velocity v_f (and also negative ions, if present) are progressively retarded and stopped from reaching the plate by the potential gradient in the ion sheath. The positive ions carry on at the drift velocity v_f and reach the plate electrode which collects a net positive current. With increasing bias voltage, the positive current rises to a steady saturation value given by $i_+ = eAn_+v_f$ when all the negative charged particles are repelled; e is the electronic charge. Normally, a negative bias of 10–20 V is sufficient; –50 V used in these measurements is more than adequate to achieve saturation. Since A and v_f are known (see Table 1), the expression for the saturation current gives a wonderfully simple and accurate means of measuring the absolute density n_+ of positive ions in the flame at the plate electrode by a routine current measurement. Very roughly, a current of 1 μA corresponds to a charged particle density of 5×10^{15} ions m^{-3} . The application of the bias voltage of –50 V does not change the ion distribution in the bulk flame plasma [12].

For the measurement of profiles of the saturation current i_+ (giving n_+) vs. distance z (0–30 mm) along the flame axis (at fixed bias voltage = –50 V) the burner was mounted on a motor-driven carriage with digital read-out of the axial distance. The designation of $z = 0$ is arbitrarily taken as a fixed distance between the burner face and the plate; in practice, the plate electrode is located just downstream of the luminous reaction zone when $z = 0$. The profiles were recorded in real time on an XY-plotter and subsequently

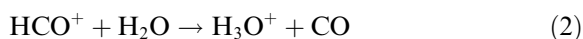
scanned into a personal computer for data analysis.

3. Results and discussion

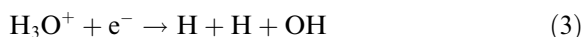
The $\text{H}_2\text{--O}_2\text{--N}_2$ flames contain very little natural ionization. When a small amount of a hydrocarbon such as methane CH_4 is introduced, ions are produced by the well-known chemi-ionization reaction [1,2]



with subsequent proton transfer to the major water product



The methane is completely consumed so that ion production is essentially switched off just downstream of the reaction zone leaving a high super-equilibrium concentration of H_3O^+ which subsequently decays throughout the burnt gas by electron–ion recombination



Such a profile is given in Fig. 1a for flame 2 doped with 2.67×10^{-3} mol fraction of CH_4 .

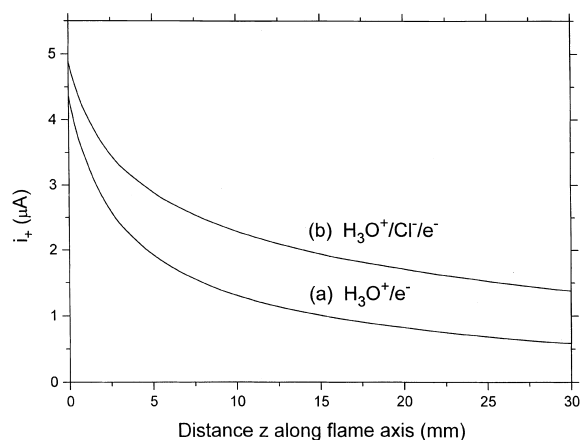


Fig. 1. Profiles of the positive ion current collected by the plate electrode vs. distance z along the axis of flame 2 doped with: (a) 2.67×10^{-3} mol fraction of CH_4 showing $\text{H}_3\text{O}^+/\text{e}^-$ recombination; and (b) 4.00×10^{-3} mol fraction of C_2HCl_3 showing recombination due to both $\text{H}_3\text{O}^+/\text{e}^-$ and $\text{H}_3\text{O}^+/\text{Cl}^-$.

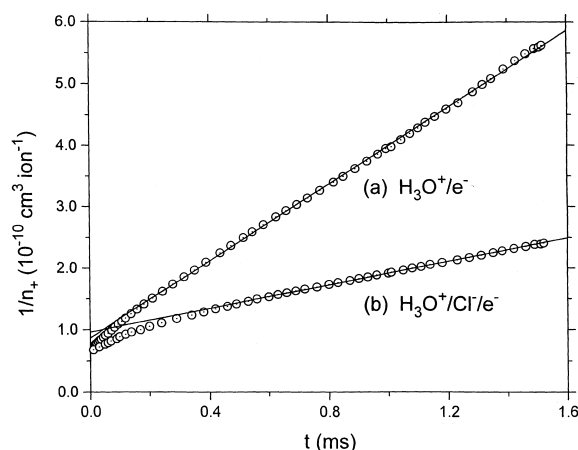


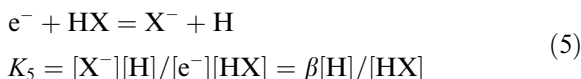
Fig. 2. Second-order recombination plots of inverse H_3O^+ ion density $1/n_+$ vs. time $t = z/v_f$ corresponding to the profiles given in Fig. 1 for flame 2 doped with: (a) 2.67×10^{-3} mol fraction of CH_4 for $\text{H}_3\text{O}^+/\text{e}^-$ recombination; and (b) 4.00×10^{-3} mol fraction of C_2HCl_3 for global recombination which includes both $\text{H}_3\text{O}^+/\text{e}^-$ and $\text{H}_3\text{O}^+/\text{Cl}^-$; the slope yields the recombination coefficient.

Since $n_+ = [\text{H}_3\text{O}^+] = [\text{e}^-]$ from quasi-neutrality, a plot of $1/n_+$ vs. time $t = z/v_f$ for the second-order reaction (3) should yield a straight line whose slope is the recombination coefficient k_3 . The corresponding plot is given in Fig. 2a; a good straight line is obtained in the range $z = 3\text{--}30$ mm giving $k_3 = (3.12 \pm 0.01) \times 10^{-7} \text{ cm}^3 \text{ molecule}^{-1} \text{ s}^{-1}$; the quoted error is ± 1 standard deviation from the linear regression.

When a halocarbon C_2HCl_3 , $\text{C}_2\text{H}_2\text{Br}_2$ or $\text{C}_2\text{H}_5\text{I}$ is added, the hydrocarbon part of the molecule produces H_3O^+ by reactions (1) and (2). The halogen X ($= \text{Cl}, \text{Br}$ or I), introduced in whatever form, exists in the flame primarily as HX and X according to the fast balanced reaction [9]:

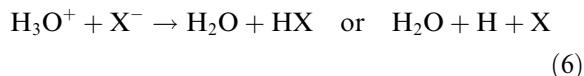


Negative ions are formed by dissociative electron attachment which is also fast and balanced [9]



The total halogen $[\text{X}]_{\text{tot}} = [\text{HX}] + [\text{X}] + [\text{X}^-] + [\text{X}^+] \simeq [\text{HX}] + [\text{X}]$ because $[\text{X}^-] \ll [\text{HX}]$ and $[\text{X}^+] \ll [\text{X}]$.

is completely negligible under the conditions of these experiments. Three-body attachment of e^- to X is much slower and can be ignored [9], even in the case of iodine where $[\text{HI}] < [\text{I}]$. Nevertheless, X^- provides a second, but slower, loss channel for H_3O^+ by ion–ion recombination



The reduced rate of recombination is shown by the profile in Fig. 1b for the same flame 2 doped with C_2HCl_3 to give 4.00×10^{-3} mol fraction of $[\text{Cl}]_{\text{tot}}$ and, as a consequence, 2.67×10^{-3} mol fraction of carbon C, the same as for Fig. 1a. Although it was not necessary, using the same mol fraction of C, with and without halogen, shows from the relative slopes that the rate of recombination decreased when halogen was added. The data from Fig. 1b are plotted in Fig. 2b as $1/n_+$ vs. t , giving a good straight line in the range $z = 8\text{--}30$ mm. The slope of Fig. 2b, smaller than that of Fig. 2a as expected, is the global recombination coefficient k_{rec} involving both reactions (3) and (6). For the general case using $[\text{H}_3\text{O}^+] = [\text{e}^-] + [\text{X}^-]$ and $[\text{X}]_{\text{tot}} = [\text{HX}] + [\text{X}]$, it is easy to formulate

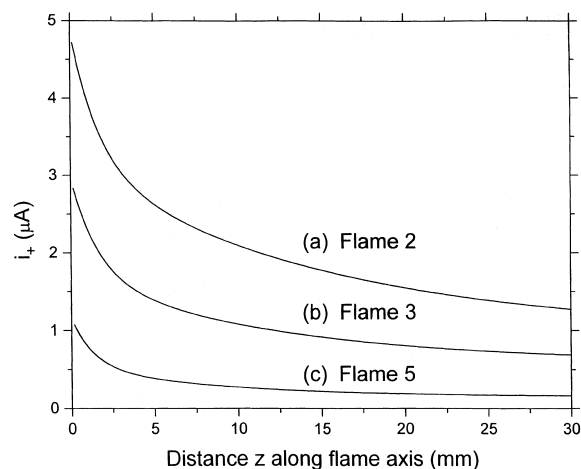


Fig. 3. Profiles of the positive ion current collected by the plate electrode vs. distance z along the axis of three flames: (a) 2 at 2400 K; (b) 3 at 2080 K; and (c) 5 at 1820 K, all doped with 2.00×10^{-3} mol fraction of $\text{C}_2\text{H}_5\text{I}$, which yield a negative temperature dependence of the recombination reaction.

$k_6 = [k_{\text{rec}}(1 + \beta) - k_3]/\beta$ with the anion/electron ratio $\beta = K_5[\text{HX}]/[\text{H}] = K_5([\text{H}_2]/[\text{H}]) \times ([\text{X}_{\text{tot}}]/([\text{H}_2] + K_4[\text{H}]))$. The equilibrium constants can be calculated at the flame temperatures from thermodynamic data in the JANAF Tables [20]; $[\text{H}_2]$ and $[\text{H}]$ are given in Table 1, obtained from a computer programme which calculates a flame's equilibrium composition of the burnt gas, also based on the JANAF Tables [20]. For example, the data in Figs. 1b and 2b for $\text{H}_3\text{O}^+/\text{Cl}^-$ recombination give $k_6 = (9.57 \pm 0.05) \times 10^{-8} \text{ cm}^3 \text{ molecule}^{-1} \text{ s}^{-1}$; here, $\beta = 4.688$, i.e., 82.42% of the negative charge is present as Cl^- .

Another aspect of interest is the dependence of the recombination coefficients on temperature. Fig. 3 shows three profiles for $\text{H}_3\text{O}^+/\text{I}^-$ recombination in (a) flame 2 at 2400 K, (b) flame 3 at 2080 K, and (c) flame 5 at 1820 K which give rate

coefficients of 7.01×10^{-8} , 9.98×10^{-8} and $13.86 \times 10^{-8} \text{ cm}^3 \text{ molecule}^{-1} \text{ s}^{-1}$, respectively. As might be expected, the values indicate a negative temperature dependence. Exactly the same procedure was followed to measure k_3 , and also k_6 with Cl, Br and I, in each of the five flames covering the temperature range 1820–2400 K. In each case, four or five determinations were carried out for each flame. For $\text{H}_3\text{O}^+/\text{e}^-$ recombination, three different CH_4 concentrations were employed for each flame, typically in the range $\approx 7 \times 10^{-4} - 4 \times 10^{-3}$ mol fraction. All of the experimental values are presented in Fig. 4; good straight lines could be drawn through the plots of $\log k$ vs. $\log T$.

The values of the recombination coefficients as a function of temperature in $\text{cm}^3 \text{ molecule}^{-1} \text{ s}^{-1}$ units are given by the expressions:

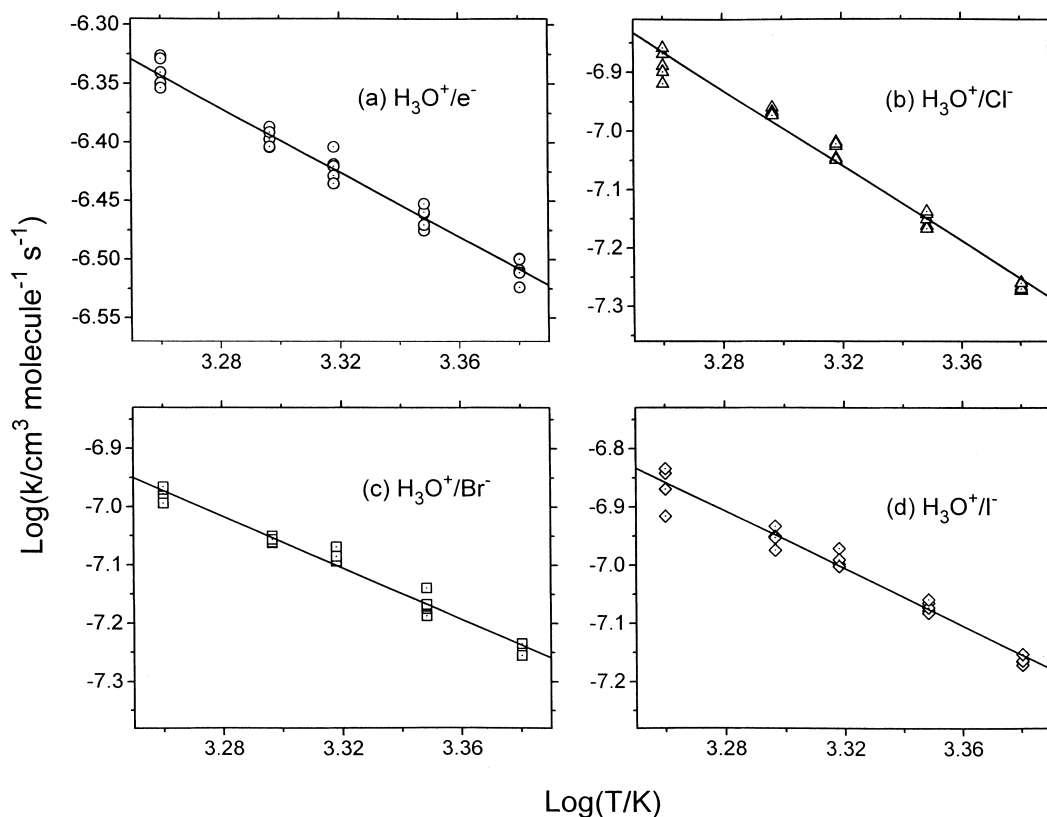


Fig. 4. Linear plots giving the temperature dependence of the rate coefficient, each for five flames in the range 1820–2400 K, for electron-ion recombination with (a) $\text{H}_3\text{O}^+/\text{e}^-$ and for ion-ion recombination with (b) $\text{H}_3\text{O}^+/\text{Cl}^-$, (c) $\text{H}_3\text{O}^+/\text{Br}^-$ and (d) $\text{H}_3\text{O}^+/\text{I}^-$.

$$k_3 = (0.0132 \pm 0.0004)T^{-1.37 \pm 0.05} \quad \text{for } \text{H}_3\text{O}^+/\text{e}^-;$$

$$k_6 = (20.8 \pm 0.7)T^{-2.52 \pm 0.16} \quad \text{for } \text{H}_3\text{O}^+/\text{Cl}^-;$$

$$k_6 = (1.01 \pm 0.04)T^{-2.14 \pm 0.07} \quad \text{for } \text{H}_3\text{O}^+/\text{Br}^-;$$

$$k_6 = (8.82 \pm 0.35)T^{-2.40 \pm 0.12} \quad \text{for } \text{H}_3\text{O}^+/\text{I}^-.$$

The error quoted on the T^n factor is the standard deviation from the straight line plots in Fig. 4. The error on the constant pre-temperature factor is the standard deviation of the data points for the flame exhibiting the greatest deviation from the mean. As an example for a mid-range temperature of 2100 K, the corresponding values are 3.71×10^{-7} , 8.83×10^{-8} , 7.85×10^{-8} and $9.38 \times 10^{-8} \text{ cm}^3 \text{ molecule}^{-1} \text{ s}^{-1}$, respectively.

In the temperature range 1820–2400 K, our values of k_3 for $\text{H}_3\text{O}^+/\text{e}^-$ recombination are within 8% of those measured by Butler and Hayhurst [3] except at the low-temperature end. Our $T^{-1.4}$ temperature dependence agrees well with the $T^{-1.5}$ factor predicted by Bardsley [21,22] for indirect dissociative recombination involving a polyatomic ion. For ion–ion recombination with Cl^- , Br^- and I^- , our values of k_6 are very roughly equal for all three halogens (within 13% of the mean) at a given flame temperature, but are high compared with previous measurements, particularly for I^- [9–11]. The low previous values probably reflect the experimental difficulties involved in sampling halogen-doped flames with a mass spectrometer. Our negative T^n temperature dependencies with n in the range from -2.1 to -2.5 are in good agreement with theoretical work by Gardner [22,23] ($n = -2$) and Sayers [22,24] ($n = -2.5$). However, the subject is complicated, and its discussion is well beyond the scope of this brief Letter.

Acknowledgements

Support of this work by the Natural Sciences and Engineering Research Council of Canada is gratefully acknowledged.

References

- [1] H.F. Calcote, in: Eighth Symposium (International) on Combustion, Williams & Wilkins, Pittsburgh, 1962, p. 184.
- [2] J.A. Green, T.M. Sugden, in: Ninth Symposium (International) on Combustion, Academic Press, New York, 1963, p. 607.
- [3] C.J. Butler, A.N. Hayhurst, J. Chem. Soc., Faraday Trans. 92 (1996) 707.
- [4] R. Kelly, P.J. Padley, Trans. Faraday Soc. 66 (1970) 1127.
- [5] L.N. Wilson, E.W. Evans, J. Chem. Soc. 46 (1967) 859.
- [6] S.D.T. Axford, A.N. Hayhurst, J. Chem. Soc., Faraday Trans. 91 (1995) 827.
- [7] H.F. Calcote, S.C. Kurzius, W.J. Miller, in: 10th Symposium (International) on Combustion, The Combustion Institute, Pittsburgh, 1965, p. 605.
- [8] A.N. Hayhurst, N.R. Telford, J. Chem. Soc., Faraday Trans. I 70 (1974) 1999.
- [9] N.A. Burdett, A.N. Hayhurst, J. Chem. Soc., Faraday Trans. I 72 (1976) 245.
- [10] N.A. Burdett, A.N. Hayhurst, C. Morley, Chem. Phys. Lett. 25 (1974) 596.
- [11] C.C.Y. Chow, J.M. Goodings, Int. J. Mass Spectrom. Ion Processes 153 (1996) 49.
- [12] J.M. Goodings, J. Guo, A.N. Hayhurst, S.G. Taylor, Int. J. Mass Spectrom. (submitted).
- [13] S.D.T. Axford, J.M. Goodings, A.N. Hayhurst, Combust. Flame 114 (1998) 294.
- [14] R.M. Clements, P.R. Smy, J. Phys. D 26 (1993) 1916.
- [15] J. Dawe, S.A.H. Rizvi, P.R. Smy, IEEE Trans. Plasma Sci. 21 (1993) 202.
- [16] C.H. Su, S.H. Lam, Phys. Fluids 6 (1963) 1479.
- [17] S.H. Lam, AIAA J. 2 (1964) 256.
- [18] J.M. Goodings, C.S. Hassanali, Int. J. Mass Spectrom. Ion Processes 101 (1990) 337.
- [19] J.M. Goodings, C.S. Hassanali, P.M. Patterson, C. Chow, Int. J. Mass Spectrom. Ion Processes 132 (1994) 83.
- [20] M.W. Chase Jr., C.A. Davies, J.R. Downey Jr., D.J. Frurip, R.A. McDonald, A.N. Syverud, JANAF Thermochemical Tables, 3rd edn., J. Phys. Chem. Ref. Data 14 (1985) (Suppl. 1).
- [21] J.N. Bardsley, Chem. Phys. Lett. 1 (1967) 229.
- [22] J.B. Hasted, Physics of Atomic Collisions, Butterworths, London, 1964, pp. 254–277.
- [23] M.E. Gardner, Phys. Rev. 53 (1938) 75.
- [24] J. Sayers, Proc. R. Soc. London, Ser. A 169 (1938) 83.